# Localization and fractality in disordered Russian Doll model

Vedant Motamarri[1,2], Alexander S. Gorsky[3,4], and Ivan M. Khaymovich[1,5,6,*]

**1** Max-Planck-Institut für Physik komplexer Systeme, Nöthnitzer Straße 38,
01187-Dresden, Germany
**2** Indian Institute of Technology Bombay, Mumbai, India 400076
**3** Institute for Information Transmission Problems RAS, 127051 Moscow, Russia
**4** Moscow Institute for Physics and Technology, Dolgoprudny 141700, Russia
**5** Institute for Physics of Microstructures, Russian Academy of Sciences, 603950 Nizhny
Novgorod, GSP-105, Russia
**6** Nordita, Stockholm University and KTH Royal Institute of Technology Hannes
Alfvéns väg 12, SE-106 91 Stockholm, Sweden
* ivan.khaymovich@gmail.com

June 2, 2022

## Abstract

Motivated by the interplay of Bethe Ansatz integrability and localization in a Richardson model of superconductivity, we consider a time-reversal symmetry breaking deformation of this model, known as a Russian Doll Model (RDM) by implementing diagonal on-site disorder. The localization and ergodicity-breaking properties of a single-particle spectrum are analyzed within a large-energy renormalization group (RG) over the momentum-space spectrum. Based on the above RG, we derive an effective Hamiltonian of the model, discover a fractal phase of non-ergodic delocalized states, with the fractal dimension different from the one of a paradigmatic Rosenzweig-Porter model, and explain it both in terms of the developed RG equations and matrix-inversion trick.

## Contents

# 1   Introduction

The Richardson model of superconductivity [1, 2] is a suitable toy model with finite number of degrees of freedom which allows to capture the key properties of superconducting state in a relatively simple manner. This model given by on-site diagonal potential $\varepsilon_n$ on $N$ sites and all-to-all constant coupling $j_{mn} = const/N$ is known to be Bethe-Ansatz (BA) integrable, where the BA equations coincide with the ones for the twisted $SU(2)$ Gaudin model [3]. The commuting integrals of motion (Hamiltonians) emerging from BA in the Richardson model get identified as superpositions of the Gaudin Hamiltonians.

The relation of integrability to localization properties of the Richardson model with diagonal on-site disorder has been considered in [4,5] using the example of a single-particle sector of the model, where it was shown that all (except one) eigenstates are localized for any coupling constant $j_{mn} \ll N^{-1}$ ($j_{mn} \gg N^{-1}$). The delocalization of the only level appears at the same coupling $j_{mn} \simeq N^{-1}$, when the superconducting gap in the many-body sector starts to be extensive. Though all (except one) eigenstates are localized for any coupling due to the BA integrability, the corresponding level statistics shows level repulsion for $j_{mn} > N^{-1}$, which is comparable with the one in the random matrix theory of Gaussian random ensembles [6]. This shows non-trivial relation of BA integrability to the localization properties already at the single-particle level.

As the Anderson localization based on the interference effects is highly sensitive to the magnetic field, it is of particular interest to go beyond the Richardson model by keeping BA integrability and at the same time break time-reversal symmetry (TRS). Such an integrable deformation of the Richardson model is called Russian Doll model (RDM) [7,8]. Like in the Richardson model, RDM has all-to-all constant coupling $j_{mn} = [g + ih\text{sign}\,(m - n)]/N$, but now it has not only a symmetric real term $\sim g$, but also an antisymmetric imaginary contribution $\sim ih\text{sign}\,(m - n)$. In this case, the BA equations for the spectrum are identical to the ones for the twisted inhomogeneous XXX $SU(2)$ spin chain. The inhomogeneous magnetic field in this model is associated with the on-site potential of RDM model, while the twist is the counterpart of the coupling constant in RDM. The TRS breaking parameter $h$ in RDM is identified as the "Planck constant" in XXX spin chain which vanishes in the Gaudin limit [9]. This model can be also related to the Chern-Simons theory when the excitations are represented by the vertex operators [10]. The RDM serves as the example of a cyclic RG when the TRS breaking parameter provides the period of a cycle, see [11]

for the review.

In this paper, motivated by the interplay of the BA integrability, localization, and level repulsion in the Richardson model, we consider the Russian Doll model bringing TRS breaking to the game, with diagonal disorder. As in the previous localization studies of the Richardson model, we focus on the single-particle sector of the RDM which still have much in common with the many-body ones, including the tower of high-energy ground state solutions.

We also consider the generalization of RDM in terms of the scaling of the coupling constant (similarly to fully-correlated cases in [12–14]). Indeed, in the original RDM the coupling in matrix Hamiltonian scales as $N^{-1}$, while we consider more general scaling $N^{-\gamma/2}$ given by the analogy with the so-called Rosenzweig-Porter model [15]. The latter is also given by the all-to-all hopping term, but each coupling is given by i.i.d. Gaussian random number with the standard deviation $N^{-\gamma/2}$.

This Rosenzweig-Porter model is known to host an entire phase of non-ergodic (so-called fractal) eigenstates in the range $1 < \gamma < 2$, squeezed between the ergodic ($\gamma < 1$) and Anderson localized ($\gamma > 2$) phases [16]. This phase is characterized by the only energy scale $\Gamma$, large compared to the level spacing $\delta \sim 1/[N\rho(E)]$ and small compared to the bandwidth $\sim 1/\rho(E)$ of the spectrum, where $\rho(E)$ is the density of states. This energy scale is given by the standard Fermi's Golden rule formula

$$\Gamma = \frac{2\pi}{\hbar} \rho(E) \sum_m |j_{mn}|^2 \sim \delta N^D \tag{1}$$

and it determines the fractal dimension $0 < D = 2 - \gamma < 1$ of the wave-function support set. Later, several other models with similar fractal [12–14,17,18] and multifractal [19–24] phases has been suggested in the literature. In all the cases it has been shown that the wave-function structure in these models is mostly determined by the diagonal elements, while the hopping terms provide a certain Breit-Wigner level broadening $\Gamma$. [1].

For Richardson model, the standard Fermi's Golden rule result fails to describe the localization properties correctly due to the presence of the strong correlations between the coupling of different sites. In the case of localization, which survives for any coupling strength even beyond the convergence of the locator expansion (like in the Richardson model [4,5] and some other long-range fully correlated models [26,27]), one can use a so-called matrix-inversion trick [12] or develop a strong-disorder spatial RG [28,29].

For RDM, in this work we show that the increasing coupling does lead to the delocalization of most of the eigenstates, therefore both above methods working only in the localized phase are not applicable. At the same time, the standard Fermi's Golden rule approximation (1) fails due to the strongly correlated coupling terms. Therefore our goal here is to develop another analytical method to describe localization and ergodicity-breaking properties of RDM. We base our approach on the RG flow, similar in spirit to the one used for disorder-free RDM for $\gamma = 2$ [7], but generalize it to the momentum space. In order to double check the RG approximations, we also generalize the above-mentioned matrix-inversion trick to the case of any divergent spectrum of the disorder-free coupling term $j_{mn}$ and show that the effective Hamiltonian obtained by this method is statistically equivalent to the one calculated from the RG flow.

By going back to the coordinate basis we derive the effective Hamiltonian with the significantly reduced correlations, which is already tractable with the Fermi's Golden rule approximation (1). The effective Hamiltonian provides the possibility to elaborate the localization properties of the single-particle states. Using combination of the effective Hamiltonian and the Fermi's Golden rule, we have found that single-particle eigenstates

---

[1] Moreover this works also for the non-Hermitian Rosenzweig-Porter model [25], where the phase diagram is affected only by the non-Hermiticity of the diagonal matrix entries, but not by hopping terms.

in the disordered RDM demonstrate fractal properties emerging in the same Anderson localization point $\gamma = 2$ as the ones in the Rosenzweig-Porter model. However, the non-ergodic phase prolongs to smaller values of $\gamma$ until $\gamma = 0$ and the corresponding fractal dimension $D$, which we exactly determine analytically, deviates from the one in the Rosenzweig-Porter and equals to $D = 1 - \gamma/2$.

The remainder of the paper is organized as follows. In Sec. 2 we explicitly describe the disordered Russian Doll model. Next, in Sec. 3 we calculate the spectrum of the disorder-free RDM, describe it in terms of energy stratification [14], and calculate the localization properties of the energy-stratified states in the momentum basis. In Sec. 4 we derive an effective Hamiltonian representation for RDM using the developed high-energy RG in the momentum space. Section 5 represents the generalization of the matrix-inversion trick invented in [12] in order to make it applicable to the description of the delocalized states and confirm its equivalence to the above RG by comparing the results for the effective Hamiltonian. In Sec. 6 we provide the analytical results leading from the structure of the effective Hamiltonian supported by numerical simulations. The conclusion and outlook are given in Sec. 7.

## 2  Model

In this work we focus on the single-particle sector of the Russian Doll model with the on-site disorder $\varepsilon_n$ and the generalized coupling amplitude $j_{mn} \sim N^{-\gamma/2}$, which can be written as the $N \times N$ random matrix of the following form in the coordinate basis $1 \leq m, n \leq N$

$$H_{mn} = \delta_{mn}\varepsilon_n - j_{mn}, \quad j_{mn} = \frac{g + ih\,\text{sign}\,(d(m,n))}{N^{\gamma/2}} \ . \tag{2}$$

Here the generalized coupling term $j_{mn}$ scales as a power $-\gamma/2$ of the system size $N$ and the on-site disorder $\varepsilon_n$ is given by Gaussian i.i.d. random variables with zero mean and the following variance

$$\langle \varepsilon_n \rangle = 0, \quad \langle \varepsilon_n^2 \rangle = W^2 \ . \tag{3}$$

The above-mentioned symmetric coupling $g$ and TRS breaking parameter $h$ are parameterized by the angular variable $\theta$ as follows

$$g = \cos\theta, \quad h = \sin\theta \ , \quad 0 \leq \theta < 2\pi \ . \tag{4}$$

For simplicity we consider the periodic boundary conditions and define the distance $d(m,n)$ with the sign: if the shortest distance from $m$ to $n$ is clockwise (counterclockwise), it is positive (negative), Fig. 1,

$$d(m,n) = (m - n) \mod N, \quad |m - n| \leq N/2 \ . \tag{5}$$

This allows us to determine an effective magnetic flux $\theta$, threading the loop $m - n - m$ and equal for each link between any pair of sites $m$ and $n$.

Note that according to the generic principles of Anderson localization in long-range models, i.e., the Anderson resonance counting [12, 16, 30, 31], the measure one of the states in this model are localized for $\gamma > 2$, irrespectively to *any* correlations or TRS breaking. This leads to the fact that all the properties of the Richardson or Rosenzweig-Porter model at $\gamma > 2$ – starting from the Lorentzian power-law profile of the eigenstates vs $\varepsilon_i$ (sometimes called frozen multifractality) and ending by the Chalker power-law scaling of the wave-function overlap, absent in the short-range Anderson models – are also present in the disordered Russian Doll model. Therefore in the further sections we will focus on the range $0 < \gamma < 2$ (if not mentioned otherwise).
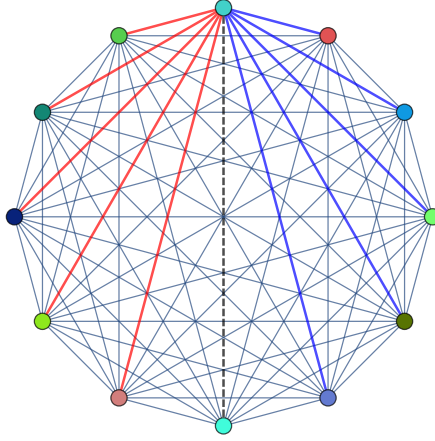
Figure 1: **Sketch of the Russian doll model, Eqs. (2)-(4).** Different colors of vertices stand for the disorder potential $\varepsilon_n$, while the coloring of the edges from the topmost vertex demonstrate different phases of hopping terms with the same amplitude: red color stands for $e^{i\theta}$, blue – for $e^{-i\theta}$, and black dashed line corresponds to the real hopping 1.

## 3    Energy stratification of the spectrum and ergodicity-breaking in momentum space

In this section we focus on the spectrum of the disorder-free RDM and, using the property of its stratification, analyze the localization and ergodicity-breaking properties of the high-energy eigenstates of the corresponding disordered RDM in the basis of the hopping term only. Indeed, the hopping term $j$ is translation invariant $j_{mn} = j_{m-n}$ therefore it can be diagonalized in the basis of plane waves

$$|p\rangle = \sum_n \frac{e^{\frac{2\pi i n p}{N}}}{\sqrt{N}} |n\rangle \ , \tag{6}$$

with the spectrum indexed by an integer $|p| \leq N/2$

$$E_0 = N^{1-\gamma/2} \cos\theta \tag{7a}$$

$$E_{2k \neq 0} = \begin{cases} 0, & \text{even } N \\ -N^{-\gamma/2} \sin\theta \tan\left(\frac{\pi k}{N}\right), & \text{odd } N \end{cases} \tag{7b}$$

$$E_{2k+1} = \begin{cases} 2N^{-\gamma/2} \sin\theta \cot\left(\frac{\pi(2k+1)}{N}\right), & \text{even } N \\ N^{-\gamma/2} \sin\theta \cot\left(\frac{\pi(2k+1)}{2N}\right), & \text{odd } N \end{cases} \tag{7c}$$

From this spectrum one can immediately see that

- For the Richardson model, $\theta = 0$, the spectrum is $(N-1)$-fold degenerate, $E_{p\neq0} = 0$, with the only finite-energy level $E_0 \sim N^{1-\gamma/2}$. It is this level which is responsible for the localization of the rest $N - 1$ eigenstates orthogonal to it in the disordered Richardson model at $\gamma < 2$ [4, 5].

- Even in the general case of $\theta \neq 0$, the levels, with non-zero even $p = 2k$, still stay small $|E_{2k}| < N^{-\gamma/2}$ (zero) for odd (even) $N$. Later we will focus on the case of even $N$ in order to neglect small amplitude of these levels. However, the levels, with odd

$p = 2k + 1$, for any finite $\theta$ immediately emerge to be as significant as $E_0$ and given for $|k| \ll N$ by

$$E_{2k+1} \sim \sin\theta \frac{2N^{1-\gamma/2}}{\pi(2k+1)} . \tag{8}$$

Note that the transition between Richardson model and RDM (see the above cases) occurs at the values of the TRS breaking parameter going to zero at $N \to \infty$, $\theta_c \sim WN^{-(1-\gamma/2)} \to 0$., It is the point, when the maximal of energies $E_{2k+1}$, namely $E_1$, goes below the diagonal disorder amplitude $W$ and therefore becomes hybridized with the rest zero modes by the diagonal disorder.

This makes the Richardson model to be an exceptional point, leading to the discontinuity between the behavior of RDM at $\theta \to 0$ and the Richardson model at $\theta \equiv 0$ in the thermodynamic limit $N \to \infty$ [2]. Another special point of $\theta = \pi/2$ is continuous as the only level $E_0 = 0$ goes to zero at that value.

In the many-body sectors of the Richardson and RDM models there is one BCS-like ground state or a whole hierarchy of such states, where the gap from these states to the rest becomes extensive at $\gamma < 2$. The single-particle sectors of these models demonstrate the same structure of gaped or energy stratified levels, even the number of these states scales with the system size $N$ in the same way. In the Richardson model (or some other long-range fully correlated models [26–28]) as well as in RDM, the energy stratified levels are special: they form a measure zero of all the spectral states, but give the main contribution to the hopping term $j_{mn}$. The most high-energetic of these states are barely affected by the disorder term and, thus, stay non-ergodic in the momentum basis due to the extensive diagonal energy there. This leads both to the ergodicity of these modes in the real space and to the main contribution of them to the hopping term.

Indeed, the disorder term $\varepsilon_n$ (3) in the momentum space basis (6) plays a role of the hopping between plane waves with the translation-invariant Gaussian i.i.d. amplitudes $J_{p-q} = \frac{1}{N}\sum_n e^{\frac{2\pi i np}{N}}\varepsilon_n$ with zero mean and the variance scaling down with the system size

$$\langle J_p \rangle = 0, \quad \langle J_p^2 \rangle = \frac{W^2}{N} . \tag{9}$$

Thus, the corresponding representation of RDM in the momentum space looks like a translation-invariant case of the Rosenzweig-Porter ensemble with a certain special realization $E_p$ of the diagonal disorder. For this model introduced in [12] it is known that the Fermi's Golden rule is applicable and gives the following broadening

$$\Gamma_p = \frac{2\pi}{\hbar}\rho(E_p)\sum_p |J_{p-q}|^2 \sim \rho(E_p)W^2 \tag{10}$$

of the Breit-Wigner approximation for the eigenstate (see, e.g., [19, 32, 33])

$$|\psi_{E_p}(p')|^2 \sim \frac{C}{(E_p - E_{p'})^2 + \Gamma_p^2} . \tag{11}$$

Here $C$ is an unimportant normalization constant and we labelled the high-energy eigenstates with disorder-free energy $E_p$ assuming smallness of the broadening $\Gamma_p$ with respect to it. One should note that, unlike the Rosenzweig-Porter model, RDM in the momentum space has highly inhomogeneous density of states (DOS) $\rho(E_p)$, $p = 2k + 1$, given by

$$\rho(E_p) \simeq \left|\frac{dp}{dE_p}\right| \sim \min\left(\frac{\pi p^2}{4\sin\theta N^{1-\gamma/2}}, \frac{1}{W}\right) , \tag{12}$$

---

[2]The similar discontinuous character of the limit is known for the Richardson model in a different class of deformations [12, 27],related to the power-law decaying hopping term $j_{mn} = 1/d(m,n)^a$ called the Burin-Maksimov model [26]

where we have taken into account that the disorder $\varepsilon_n \sim W$ hybridizes the levels as soon as the disorder-free version of DOS $|dp/dE_p|$ goes above its bare disorder counterpart $|dn/d\varepsilon_n| \sim 1/W$.

The support set $\Delta p$ occupied by the eigenstate (11) in the momentum space can be found from the condition

$$|E_{p+\Delta p} - E_p| \simeq \Gamma_p \ , \tag{13}$$

which leads to the non-ergodic behavior as soon as $\Delta p \propto N^{D(p)}$ scales as a fractional $D(p) < 1$ power of $N$.

As soon as $|E_{p+\Delta p} - E_p| \simeq |E_p|$ (or $\Delta p \simeq p$), the condition (13) with substituted (8), (10), and (12) leads to the number $p^*$ of energy-stratified states which are non-ergodic in the momentum basis:

$$p^* \simeq \frac{2}{W} \frac{\sin\theta}{\pi} N^{1-\gamma/2} \ , \quad \Gamma_{p^*} \simeq W \ . \tag{14}$$

The energies of these states are barely affected by disorder, as $E_p$ are extensive, $E_p \gg W$ at $|p| \ll p^*$. Thus, our criterion is consistent to the so-called Mott's principle (see, e.g., [12]), claiming that as soon as the bare diagonal energy $E_p$ of the state is large compared to the spectral width $W$ of the hopping term $J_{p-q}$, this state is non-ergodic in the corresponding (momentum) basis. Note that at $\theta < \theta_c \sim N^{-(1-\gamma/2)}$ only the state $p = 0$ is non-ergodic (localized) in the momentum space. Note also that the support set $\Delta p$ is limited from above by $p < p^* \sim N^{1-\gamma/2}$. Thus, from the condition $D(p) < 1$ Eq. (14) is valid until $p^* \ll N$, i.e. for $\gamma > 0$. Further we will mostly focus our consideration to this parameter interval, $0 < \gamma < 2$.

# 4  Large energy RG in the momentum space. Effective Hamiltonian

In the paper [7], the authors consider the RG flow over the matrix size $N$ in clean RDM, with the linearly increasing diagonal terms $\varepsilon_n \sim n$, where each RG step was represented by the removing of one row and one column corresponding to the largest diagonal element $\varepsilon_N$. In particular, they perform the following steps:

1. First, they start with the matrix of size $N_0$ and at each step reduce its size by one.

2. For this, they take at each step the highest diagonal energy in the absolute value ($\varepsilon_N$ or $\varepsilon_1$) and assuming it to be large with respect to the rest of the levels and with respect to the hopping terms

$$|\varepsilon_N| \gg j_{Nn} \ , \tag{15}$$

they resolved the eigenproblem with respect to the site $i = N$ corresponding to this level $\varepsilon_N$:

$$(\varepsilon_m - E)\,\psi_E(m) - \sum_n j_{mn}\psi_E(n) = 0 \tag{16a}$$

$$\psi_E(N) = \frac{\sum_{n \neq N} j_{Nn}\psi_E(n)}{\varepsilon_N + j_{NN} - E} \tag{16b}$$

$$(\varepsilon_m - E)\,\psi_E(m) - \sum_{n \neq N} j_{mn}(1)\psi_E(n) = 0 \ , \tag{16c}$$

where $m \neq N$ and $j_{mn}(1)$ is calculated by one RG step

$$j_{mn}(r+1) = j_{mn}(r) + \frac{j_{mN}(r)j_{Nn}(r)}{\varepsilon_N + j_{NN}(r) - E} \ , \tag{17}$$

with $j_{mn}(0) = j_{mn}$.

3. Next, they assumed $\varepsilon_N + j_{NN} - E \sim W$ and using the ratio $W/\delta = N$ they end up in cyclic RG equations.

In the disordered RDM the above consideration fails as the maximal diagonal matrix element does not correspond to the maximal (or minimal index) which breaks down the self-similar structure of the matrix at further RG steps (see, e.g., [34]). However, analogously to the renormalization group (17) considered in [7], one can take into account the large diagonal terms in the *momentum* basis, with the diagonal energies $E_p$ (7) and the hopping terms $J_{p-q}$ (9) satisfying similar inequality to (15)

$$|E_p| \gg |J_{p-q}| . \tag{18}$$

The corresponding equation for a certain $r$th step for the momentum $p_r$ is given by the following hopping term renormalization step

$$J_{p,q}(r+1) = J_{p,q}(r) + \frac{J_{p,p_r}(r)J_{p_r,q}(r)}{E_{p_r} + E - J_{p_r,p_r}(r)} , \tag{19a}$$

$$J_{p,q}(0) = J_{p-q} , \tag{19b}$$

while the diagonal term stays the same

$$E_q(r) = E_q \text{ for } q \neq p_1, \ldots, p_r . \tag{20}$$

Of course such renormalization works only when Eq. (18) is valid, i.e. at least for $\gamma < 3$, which is the case in our interval of the interest, $0 < \gamma < 2$.

Further we will remove the largest $E_p$ in the following order for $s$ up to $s = r \leq N/4$

$$p_0 = 0, \quad p_{2s-1} = -(2s-1), \quad p_{2s} = 2s - 1 . \tag{21}$$

Here we should warn a reader that both $\theta = 0$ and $\theta = \pi/2$ has been considered (slightly) differently. As for the vicinity of the Richardson model, $\theta \lesssim N^{-(1-\gamma/2)}$, the only level satisfying (18) is $E_0$, we can consider only one renormalization step $r = 1$. For the vicinity of $\theta = \pi/2$, on the contrary, $E_0$ is the level which invalidates (18), thus we should start with $s = 1$. However, as we will see in Eqs. (27) and (31) the latter does not change the results.

In the following, we plan to find the optimal number of RG steps needed for writing the effective Hamiltonian for the bulk spectral states, $E \sim O(1)$, with suppressed correlations. The effects of the energy-stratified states will be taken into account by RG. In order to find the effective Hamiltonian, in the next subsection 4.1 we, first, simplify the RG flow (19) focusing on the leading contributions by the order of magnitude. Next, in the following subsection 4.2 we rewrite the Hamiltonian in the coordinate basis in order to find the optimal number $r$ of RG steps needed for minimization of the broadening $\Gamma$ found by the Fermi's Golden rule from the effective Hamiltonian.

## 4.1 Simplification of RG (19)

In order to simplify the RG flow (19) here we show that the main contribution to it is given by

$$\bar{J}_{p,q}(r+1) = J_{p-q} + S_{p,q}(r) , \tag{22}$$

where

$$S_{p,q}(r) = \sum_{k=0}^{r} \frac{J_{p-p_k}J_{p_k-q}}{E_{p_k} + E - J_{p_k-p_k}} . \tag{23}$$

Indeed, this takes into account the renormalization (19) itself, but neglects the renormalization of the hopping terms $J_{p,q}(r)$ in the sum $S_{p,q}(r)$.

As we show in Appendix A for all $r$ smaller than

$$r \ll r^{**} = N^{1-\gamma/3} \tag{24}$$

the above approximation works leading to $|S_{p,q}(2r)| \ll |J_{p-q}|$ and the difference between $J_{p,q}$ and $\bar{J}_{p,q}$ at most of the order of $|S_{p,q}|$.

Note that the value $r^{**}$ corresponding to the momentum value $p^{**} = 2r^{**} - 1 \gg p^*$ according to Eq. (21) is large compared to the number $p^*$ of energy-stratified states (14) at $\gamma > 0$. Thus, one can take into account all the high-energy states within the above RG flow.

## 4.2  Effective model in the coordinate basis.

Now we are in the position to calculate effective renormalized model (20) and (22) in the coordinate basis in order to further estimate the fractal dimension of the eigenstates in the coordinate basis.

For this purpose we separate our renormalized Hamiltonian in four terms

$$
\begin{aligned}
H_{p,q}(2r) \quad &= J_{p-q} + \frac{J_p J_{-q}}{E_0} \quad + \sum_{l=1}^{r} \frac{a_{p,q,l}}{E_{2l-1}} + E_q \delta_{p,q} \equiv \\
&\equiv H_{p,q}^{(1)} + H_{p,q}^{(2)} \quad + \quad H_{p,q}^{(3)} \quad + \quad H_{p,q}^{(4)} ,
\end{aligned}
\tag{25}
$$

where $a_{p,q,l} = J_{p-2l+1} J_{2l-1-q} - J_{p+2l-1} J_{-2l+1-q}$ and $p,q \neq p_s$, with $0 \leq s \leq r$, and $p_s$ are from Eq. (21).

The discrete Fourier transform of the above terms takes the form

$$
H_{m,n}^{(k)} = \sum_{p,q \neq \{p_s\}} \frac{e^{\frac{2\pi i(pm-qn)}{N}}}{N} H_{p,q}^{(k)} = \left( \sum_{p,q} + \sum_{p,q=\{p_s\}} - \sum_{\substack{p,\\q=\{p_s\}}} - \sum_{\substack{p=\{p_s\},\\q}} \right) e^{\frac{2\pi i(pm-qn)}{N}} H_{p,q}^{(k)} ,
\tag{26}
$$

where we replaced the summation over $p, q \neq \{p_s\}$ by the complemented sums over the whole interval and over $p_s$ in either or both variables. The first summation is given just by the initial (not truncated) Fourier transform.

After straightforward algebra and neglecting subleading corrections (both given in Appendix B), one obtains the following renormalized Hamiltonian in the coordinate basis at $2r$th step of RG flow, with $1 \leq r \leq N/4$ and a certain unimportant constant $c$

$$
H_{m,n}(2r) \sim \varepsilon_m \delta_{mn} + \frac{\varepsilon_m \varepsilon_n}{N^{2-\gamma/2} \cos\theta} +
$$
$$
+ \begin{cases}
\frac{2}{\pi} N^{-\gamma/2} \sin\theta \left(1 - r\frac{m-n}{N}\right) + \frac{i8\pi^2 \varepsilon_m \varepsilon_n (m-n) r^3}{3N^{3-\gamma/2}\sin\theta} - (\varepsilon_m + \varepsilon_n)\frac{r}{N}, & |m-n| \ll \frac{N}{r} \\
\frac{2}{\pi} N^{-\gamma/2} \sin\theta \frac{c}{r} + \frac{i2\pi \varepsilon_m \varepsilon_n}{N^{2-\gamma/2}\sin\theta} \left(c\frac{N^2 \text{sign}(m-n)}{(m-n)^2} + r\right) - \frac{\varepsilon_m + \varepsilon_n}{2\pi|m-n|}, & |m-n| \gg \frac{N}{r}
\end{cases} .
\tag{27}
$$

# 5  Generalization of the matrix-inversion trick for Russian Doll model

Here we present an alternative way to derive the effective Hamiltonian of RDM in the momentum space, analogous to (25), which is free from the approximations of the above RG. For this purpose we generalize the matrix-inversion trick invented in [12].

The main idea of the matrix-inversion trick is as follows: having large eigenvalues $E_p$ of the hopping matrix elements, one adds to the hopping matrix the identity matrix multiplied by a certain constant $E_0$ and inverse this matrix as follows

$$E|\psi_E\rangle = \left( \sum_p E_p|p\rangle\langle p| + \sum_n \varepsilon_n|n\rangle\langle n| \right)|\psi_E\rangle \iff$$

$$\sum_n (E + E_0 - \varepsilon_n)|n\rangle\langle n|\psi_E\rangle = \sum_p (E_p + E_0)|p\rangle\langle p|\psi_E\rangle \iff$$

$$\sum_p \frac{1}{E_p + E_0}|p\rangle\langle p| \sum_n (E + E_0 - \varepsilon_n)|n\rangle\langle n|\psi_E\rangle = |\psi_E\rangle . \quad (28)$$

In such a way the large energies $E_p$ of the hopping matrix elements, providing the dominant contribution to the hopping, can be sent to the denominator without changing the basis, thus, the effective model can be treated with the perturbation theory as soon as the parameter $E_0$ is selected to avoid any resonances $E_p + E_0 \gtrsim O(1)$.

For the models with one-sided divergence of the spectrum $E_p$ (like in the Burin-Maksimov model [12], where $E_{p<p^*} \gg 1$ are large and positive $E_{p<p^*} > 0$) one can avoid having singularities in the denominator $E_p + E_0$ by selecting $E_0 < -\min_p E_p \sim O(1)$ and show wave-function localization.

However in RDM the spectrum is unbounded from both sides (see Eq. (8) for positive and negative $k \ll N$) and does not have finite gaps in the thermodynamic limit at finite energies in order to find $E_0 \sim O(1)$ and, thus, avoid the divergence at the inversion of $E_p + E_0$ terms.

In order to restore the convergent matrix inversion, one has to invert only *a part* of the spectrum given by high-energy levels $E_{p<p_r}$

$$E|\psi_E\rangle = \left( \sum_p E_p|p\rangle\langle p| + \sum_n \varepsilon_n|n\rangle\langle n| \right)|\psi_E\rangle \iff$$

$$\left[ \sum_n \varepsilon_n|n\rangle\langle n| + \sum_{|p|>p_r} E_p|p\rangle\langle p| \right]|\psi_E\rangle = \left[ \sum_{|p|<p_r} (E - E_p)|p\rangle\langle p| + \sum_{|p|>p_r} E|p\rangle\langle p| \right]|\psi_E\rangle \iff$$

$$\left[ \sum_{|p|<p_r} \frac{1}{1 - E_p/E}|p\rangle\langle p| + \sum_{|p|>p_r} |p\rangle\langle p| \right] \left[ \sum_n \varepsilon_n|n\rangle\langle n| + \sum_{|p|>p_r} E_p|p\rangle\langle p| \right]|\psi_E\rangle = E|\psi_E\rangle \iff$$

$$\left[ \left( \sum_{|p|>p_r} |p\rangle\langle p| + \sum_{|p|<p_r} \frac{E}{E_p}|p\rangle\langle p| \right) \sum_n \varepsilon_n|n\rangle\langle n| + \sum_{|p|>p_r} E_p|p\rangle\langle p| \right]|\psi_E\rangle = E|\psi_E\rangle , \quad (29)$$

where for simplicity we take $E_0 = -E$ and use $|E_{|p|<p_r}| \gg E$.

Eq. (29) gives the term-by-term correspondence to Eq. (25). Indeed

- the first term is equivalent to $H^{(1)}$ after neglecting subleading terms like $i_{mn}$ in (65) of Appendix B,

- the part of the second term with $p = p_0 = 0$ corresponds to $EH^{(2)}_{mn}/\varepsilon_m$ after neglecting $g_{m,0}\sqrt{r/N}$ subleading terms in (25),

- the rest part of the second term with $p = p_s \neq 0$ corresponds to $EH^{(3)}_{mn}/\varepsilon_m$ after neglecting $g_{m,0}\sqrt{r/N}$ subleading terms in (25),

- while the last term is just equal to $H^{(4)}$.

To sum up, this result shows that all the approximations performed in the previous section in order to derive the effective Hamiltonian, Eq. (27), either lead to subleading corrections or a to the prefactors $E/\varepsilon_m \sim O(1)$ of the order of unity. As the matrix-inversion trick is just another representation of the exact eigenproblem without any approximation, the equivalence between Eqs. (25) and (29) confirms the applicability of the effective Hamiltonian (27) to the whole range of parameters of interest, $0 < \gamma < 2$.

# 6  Results

Now we are ready to calculate non-ergodic properties of eigenstates based on the effective Hamiltonian (27) and Fermi's Golden rule approximation (1). Like with the matrix-inversion trick [12], the Fermi's Golden rule for each effective Hamiltonian with a certain $r$ gives an upper bound for the fractal dimension via broadening $\Gamma_n(2r)$ (see the definition below). Therefore in order to find the true fractal dimension of the problem one should make the upper bound strict by finding the minimum of $\Gamma_n(2r)$ via the optimization of the value of $r = r_{\text{opt}}$. Further we implement this algorithm analytically and verify the results for the fractal dimension numerically by calculation the eigenstate statistics.

## 6.1  Analytical results – Optimization of fractal dimension

Similarly to the Rosenzweig-Porter model, in the model given by the effective Hamiltonian (27), we expect to see only fractal (defined via level broadening in (33)), but not multifractal states (where multifractal dimensions $D_q$ are parameterized by the order $q$ of the wave-function moment, see Sec. 6.2). Therefore, in order to calculate this fractal dimension $D$ of eigenstates in RDM (2), we use the Fermi's Golden rule formula analogous to (1), but with the effective hopping term from the renormalized Hamiltonian (27)

$$\Gamma_n(2r) = \frac{2\pi}{\hbar}\rho(E_n)\sum_{m\neq n}|H_{m,n}(2r)|^2 . \tag{30}$$

Taking the energies and DOS of the bulk of the spectrum, $E_n \sim \varepsilon_n \sim W$ and $\rho(E_n) \sim 1/W$, one obtains for each term of the effective Hamiltonian the following expression [3]

$$\frac{W}{2\pi}\Gamma_n(2r) \sim \frac{W^4}{N^{3-\gamma}\cos^2\theta} + \frac{4}{\pi^2}N^{-\gamma}\sin^2\theta\left[\sum_{n=0}^{N/r}\left(1 - \frac{r}{N}n\right)^2 + \frac{c^2}{r^2}\left(N - \frac{N}{r}\right)\right] +$$

$$+ \frac{W^4}{N^{4-\gamma}\sin^2\theta}\left[\sum_{n=0}^{N/r}n^2\frac{64\pi^4 r^6}{9N^2} + \sum_{n=N/r}^{N}\frac{c^2 N^4}{16\pi^2 n^4} + r^2\left(N - \frac{N}{r}\right)\right] + W^2\left[\frac{r^2}{N^2}\frac{N}{r} + \sum_{n=N/r}^{N}\frac{1}{4\pi^2 n^2}\right] \sim$$

$$\sim \frac{W^4}{N^{3-\gamma}\cos^2\theta} + \frac{4}{\pi^2}\sin^2\theta\frac{N^{1-\gamma}}{r} + \frac{W^4 r^3}{N^{3-\gamma}\sin^2\theta} + \frac{W^2 r}{N} \tag{31}$$

The first term (corresponding to $H^{(3)}$ with $p = p_0$) is subleading for all $|\theta| \gg N^{-(1-\gamma/2)}$ and $r \gg 1$. Formally in the vicinity of $\theta = \pi/2$ this term diverges, but as we discussed after (18) that equality should be satisfied in order to write this term. In the same way, in the vicinity of $\theta = 0$ the divergence of the third term $\sim 1/\sin\theta$ is fake.

---

[3]Here we neglect the cross-terms as we are interested in the dominant contributions and the competition between them at different $r$.

After neglecting the first term for finite $\theta$, the rest three terms, except the first one, give the optimal value of $r$ corresponding to the minimal level broadening

$$r_{\text{opt}} \simeq c \frac{\sin\theta}{W} N^{1-\gamma/2} \;\Leftrightarrow\; \Gamma_n(r_{\text{opt}}) \simeq c' \sin\theta N^{-\gamma/2} \;, \tag{32}$$

with certain constants $c$ and $c'$ of the order of one. Note that this optimal point $r_{\text{opt}}$ satisfies the condition (24), $r \ll r^* \sim N^{1-\gamma/3}$, for all $\gamma > 0$. The validity condition $|J_{p,q}(r) - \bar{J}_{p,q}(r)| \ll |S_{p,q}(r)|$ for the above used RG, leading to $r \ll N^{(3-\gamma)/4}$ from Eq. (56) in Appendix A, is satisfied at $\gamma > 1$. However, even for $r \gtrsim N^{(3-\gamma)/4}$, corresponding to $0 < \gamma < 1$ the $J_{p,q}(r) - \bar{J}_{p,q}(r)$ gives at most the same-order contribution as the $S_{p,q}(r)$ and affects only the numerical prefactors $c$ and $c'$.

As in the bulk of the spectrum the mean level spacing is $\delta = 1/(\rho(E)N) \sim W/N$, the fractal dimension for the typical wave function in this case should be given by the ratio

$$N^D = \Gamma_n(r_{\text{opt}})/\delta \sim \frac{\sin\theta}{W} N^{1-\gamma/2} \;\Leftrightarrow\; D = 1 - \gamma/2 \;, \tag{33}$$

which is different from the one in the Rosenzweig-Porter model [16]. This result is also confirmed by numerical calculations below, where we define the fractal dimension via the inverse participation ratio (but not as the number of sites where the wave function has significantly non-zero values within the Breit-Wigner approximation). Note that in the case when the Fermi's Golden rule does not work for the initial problem, the number $p^*$ of the energy-stratified levels, Eq. (14), determines the fractal dimension via the expression $p^* \sim N^D$ (see [14] for more details).

The effective renormalized Hamiltonian (27) in this case is given by

$$H_{m,n}(2r_{\text{opt}}) \simeq \varepsilon_m \delta_{mn} - \begin{cases} \left(\frac{\varepsilon_m + \varepsilon_n}{W} - c\right)\Gamma, & |m-n| \ll W/\Gamma \\ \frac{\varepsilon_m + \varepsilon_n}{2\pi|m-n|}, & |m-n| \gg W/\Gamma \end{cases} \;, \tag{34}$$

where $W/\Gamma \simeq N/r_{\text{opt}} \sim (W/\sin\theta)N^{\gamma/2}$ and we neglect the subleading terms for simplicity.

Note that the Hamiltonian (34) is equivalent to the one of power-law random banded matrices [35] with a bandwidth $b$ and diagonal disorder $W$ rescaled as $\sim N^{\gamma/2}$.

- if none of $b$ and $W$ is scaled with $N$ the system hosts genuinely *multifractal* states, with $D_q \sim b$ at $b \ll 1$ and $1 - D_q \sim 1/b$ at $b \gg 1$ [35],

- The scaling $b \sim N^{\gamma/2}$, $W = O(1)$ sends the system to the ergodic phase, with $D = 1$,

- the scaling $W \sim N^{\gamma/2}$, $b = O(1)$ leads to the system localization, $D = 0$,

- while the case of RDM, corresponding to the simultaneous scaling of both parameters $W \sim b \sim N^{\gamma/2}$, gives fractal eigenstates described by the Fermi's Golden rule (30) [4].

The bulk eigenstates of such effective Hamiltonian should be given by two contributions:

- First, due to the presence of the Rosenzweig-Porter-like long-range hopping terms at $|m-n| \ll W/\Gamma$ the wave-function should have a contribution of a Lorentzian profile versus $\varepsilon_n$ with the width $|E_m - \varepsilon_n| \sim \Gamma$ [19, 32, 33]

$$|\psi_{E_m}(n)|^2 \simeq \frac{\delta\Gamma}{(E_m - \varepsilon_n)^2 + \Gamma^2} \;. \tag{35}$$

---

[4]However, there are some investigations which might have multifractal wave functions, with the fractal structure in the energy spectrum inside a miniband of size $\Gamma \sim N^{-\gamma/2}$ provided by the Fermi's Golden rule [24].

- Second, similar to the power-law banded random matrices $\langle|j_{mn}|^2\rangle \sim |m-n|^{-2a}$ at the critical power $a = 1$, there should be the multifractal proliferation of the wave-function maxima given by the resonances. However, unlike the power-law banded random matrix case, in the RDM case the $N$-scaling of the cutoff $W/\Gamma \sim N^{\gamma/2}$, at which this power-law comes into play, significantly reduces the number of resonances:

$$N_{res} \sim \sum_m |H_{mn}|/W \sim \ln\left(N\Gamma/W\right) = (1 - \gamma/2)\ln N \tag{36}$$

and do not affect the fractal dimension of the system given by (see, e.g., Eqs. (30-31) in [36])

$$D \ln N \sim N_{res} \;\Leftrightarrow\; D = 1 - \gamma/2 \; . \tag{37}$$

## 6.2 Numerical results – Spectrum of fractal dimensions, level statistics, and wave-function decay

Numerically we do not stick to any approximation, but instead consider exact diagonalization of the initial model (2) calculating the eigenstates $\psi_{E_n}(m)$ in the coordinate basis and eigenvalues $E_n$.

Focusing on the mid-spectrum states, we perform the multifractal analysis. For this purpose, we consider two relevant measures of eigenfunction statistics based on the distribution of amplitudes $P(|\psi_E(n)|^2)$.

First, we consider the *spectrum of fractal dimensions* defined as the power $f(\alpha)$ of the scaling of the distribution $P(\alpha) \sim N^{f(\alpha)-1}$ of $\alpha = -\ln|\psi_E(n)|^2/\ln N$ [37]

$$f(\alpha) = 1 - \alpha + \lim_{N\to\infty}\frac{\ln[P(|\psi_E(n)|^2 = N^{-\alpha})]}{\ln N} \; . \tag{38}$$

This $f(\alpha)$ is a kind of large deviation function showing the tails of the distribution of $\ln|\psi_E(n)|^2$ far away from its typical (most probable) value

$$\langle\ln|\psi_E(n)|^2\rangle = -\alpha_0 \ln N \; . \tag{39}$$

It has a bunch of properties (like the normalization condition of the probability distribution, $f(\alpha) \leq 1$, $f(\alpha_0) = 1$, or the wave-function normalization $f(\alpha) \leq \alpha$, $f(\alpha_1) = \alpha_1$), among which we just mention the symmetry [37]

$$f(2 - \alpha) = f(\alpha) - (\alpha - 1) \; , \tag{40}$$

relating wave-function peaks (small $\alpha < 1$) and tails (large $\alpha > 1$). This symmetry is known to work for the non-ergodic extended states, fractal or multifractal. In particular, for the Rosenzweig-Porter model, as shown in [16], $f(\alpha)$ takes a simple linear form for $\gamma \geq 1$ with an additional point $f(0) = 0$ for $\gamma > 2$

$$f_{RP}(\alpha) = \begin{cases} 1 + (\alpha - \gamma)/2, & \max(0, 2 - \gamma) < \alpha < \gamma \\ -\infty, & \text{otherwise} \end{cases} , \tag{41}$$

satisfying the symmetry (40) for $\gamma < 2$.

The second widely used probe of multifractality is the inverse participation ratio $I_q$ defined via the moments of eigenstates as follows

$$I_q = \sum_n |\psi_E(n)|^{2q} \sim N^{-(q-1)D_q} \; , \tag{42}$$
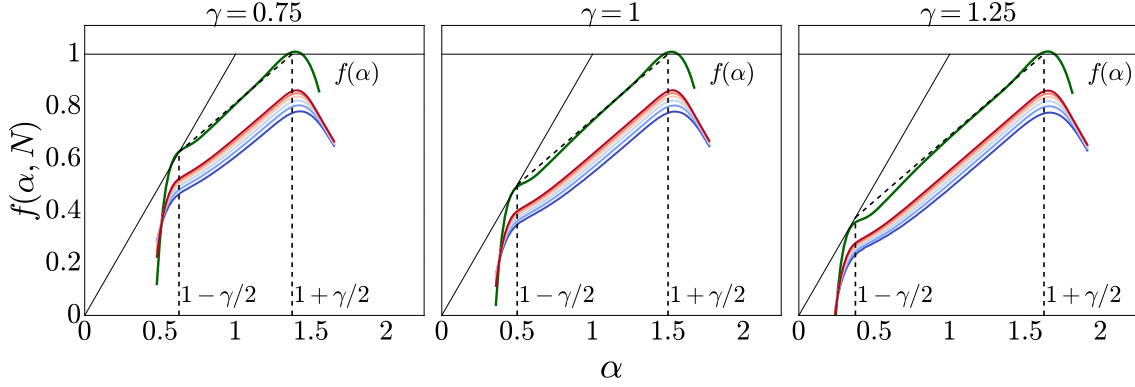
Figure 2: **The spectrum of fractal dimensions** $f(\alpha)$ in RDM model for 50 % mid-spectrum eigenstates, $\theta = 0.25$, and (left) $\gamma = 0.75$, (middle) $\gamma = 1$, and (right) $\gamma = 1.25$. $f(\alpha)$ is extrapolated (green) from $N = 2^9 - 2^{14}$ (from blue to red) with 1000 disorder realizations for each. The grey dashed line shows the analytical prediction (46).

where the $q$-dependent exponents $D_q$ are called fractal dimensions. For the ergodic states $D_q = 1$ for all $q$, while for the localized situation $D_q = 0$ for $q > 0$. The intermediate case of $0 < D_q < 1$ called non-ergodic delocalized case. In the multifractal situation, $D_q$ is represented by strictly decaying function, while in the fractal one, $D_q = D$ does not depend on $q$ at least for $q > 1/2$.

The relation between $D_q$ and $f(\alpha)$ is given by the saddle-point approximation of the disorder averages moments:

$$\langle I_q \rangle = N \int |\psi|^{2q} P(\psi) d\psi = \int_0 N^{f(\alpha) - q\alpha} d\alpha \simeq N^{\max_\alpha [f(\alpha) - q\alpha]} \tag{43}$$

and given by the Legendre transform

$$(q-1)D_q = q\alpha_q - f(\alpha_q), \text{ where } f'(\alpha_q) = q . \tag{44}$$

The last equality is just the definition of $\alpha_q$.

From the above definition one can immediately see that $\alpha_1$ determining the wave-function normalization condition $f(\alpha_1) = \alpha_1$ gives the limiting value $D_{q \to 1}$

$$D_1 = \alpha_1 = 2 - \alpha_0 , \tag{45}$$

while the latter equality is given by the symmetry (40). Here $\alpha_0$ determines the most typical wave-function coefficients (39) and gives the maximum of $f(\alpha_0) = 1$.

From the above relation and from the predicted value of the fractal dimension, Eq. (33) one can find the spectrum of fractal dimension in RDM similarly to (41)

$$f(\alpha) = \begin{cases} 1 + \frac{(2\alpha - 2 - \gamma)}{4}, & \max\left(0, 1 - \frac{\gamma}{2}\right) < \alpha < 1 + \frac{\gamma}{2} \\ -\infty, & \text{otherwise} \end{cases} , \tag{46}$$

Alternatively one can derive the above expression from the Breit-Wigner approximation (11) with the broadening (33), see, e.g., [33].

Numerically, one cannot achieve the infinite system sizes, therefore both the spectrum of fractal dimensions, Eq. (38), and the fractal dimensions themselves, Eq. (42), can be calculated only for finite systems and extrapolated to the thermodynamic limit $N \to \infty$ (see Appendix C). The spectrum of fractal dimension at finite system sizes can be extracted directly from the histogram over $\alpha$ (see, e.g., [12,16,38,39]), while the inverse participation ratio is just given by Eq. (42).
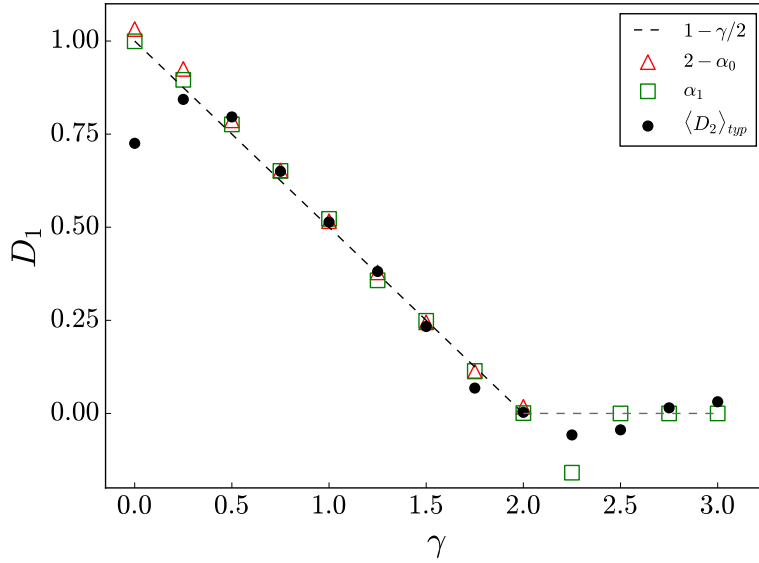
Figure 3: **The fractal dimension $D_1$ versus $\gamma$** in RDM model for 50 % mid-spectrum eigenstates, and $\theta = 0.25$. The symbols correspond to $D_q$ extracted from the inverse participation ratio ($\bullet$) and from the points corresponding to the first $\alpha_1$ ($\square$), and zeroth $2 - \alpha_0$ ($\triangle$) moments of $P(\alpha) \sim N^{f(\alpha)-1}$. The black dashed line shows the analytical prediction (33). The symmetry (40) used for $2 - \alpha_0$ works only for the delocalized phases, i.e. we plot $2 - \alpha_0$ only for $\gamma \leq 2$. The data is extrapolated from $N = 2^9 - 2^{14}$ with 1000 disorder realizations for each.

Figure 2 shows the spectrum of fractal dimensions $f(\alpha)$ extracted from the numerical simulations. One can see that the extrapolation procedure gives the correct normalization value $f(\alpha_0) = 1$ and the perfect agreement with the analytical formula (46).

Both from the inverse participation ratio (42) and from its relation to $f(\alpha)$ (45) one can extract the fractal dimension $D_1$, see Fig. 3. A perfect agreement both between each other and with the analytical prediction (33) confirms our analytical derivation and the symmetry (40) of $f(\alpha)$. Some deviations from the prediction in the localized phase are caused by the finite-size effects which are enhanced close to the Anderson transition.

Note that, according to the analytical prediction, the fractal dimension is not homogeneous across the spectrum and this is confirmed also numerically, see Fig. 4: The fractal dimension in the spectral bulk (for more than 90 % at the considered system sizes) shows the above fractal behavior for $0 < \gamma < 2$, while at the edges the high-energy states become ergodic with $D_2 \to 1$.

In addition to the previous two measures, we consider the eigenvalue statistics using a so-called adjacent level gap ratio (defined in [40,41]) and the wave-function spatial decay (first used in [27]).

The ratio statistics is given by

$$r_n = \frac{\min(s_n, s_{n+1})}{\max(s_n, s_{n+1})}, \text{ where } s_n = E_{n+1} - E_n . \tag{47}$$

The localization corresponds to the Poisson level statistics, characterized by the absence of level repulsion and leading to $r = \langle r_n \rangle = r_P = 2\ln 2 - 1 \simeq 0.3863$. The ergodic random-matrix prediction corresponds to the Wigner surmise [6] and is given by $r_{GOE} \simeq 0.5307$ for the orthogonal symmetry and $r_{GUE} \simeq 0.5996$ for the unitary one. For the fractal phase of the Rosenzweig-Porter kind the gap ratio still shows the Wigner-Dyson value in the entire
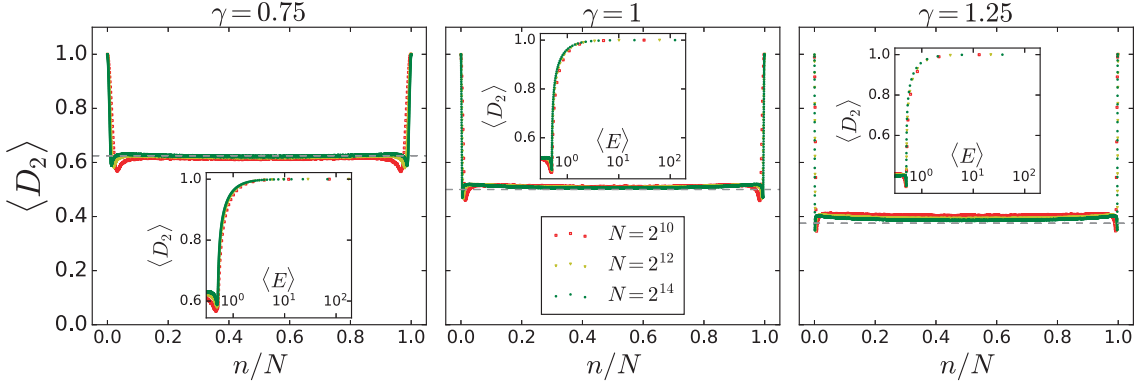
Figure 4: **The fractal dimension $D_2(E_n)$ versus energy index $n$** in RDM model for $\gamma = 0.75$, 1, 1.25, $\theta = 0.25$, and $N = 2^{10}, 2^{12}, 2^{14}$. (insets) the same data for $D_2(E_n)$, shown vs energy $E_n$ and zoomed close to the right spectral edge. The data both for $D_2(E_n)$ and $E_n$ are averaged over 1000 realizations of disorder for each eigenvalue index separately.
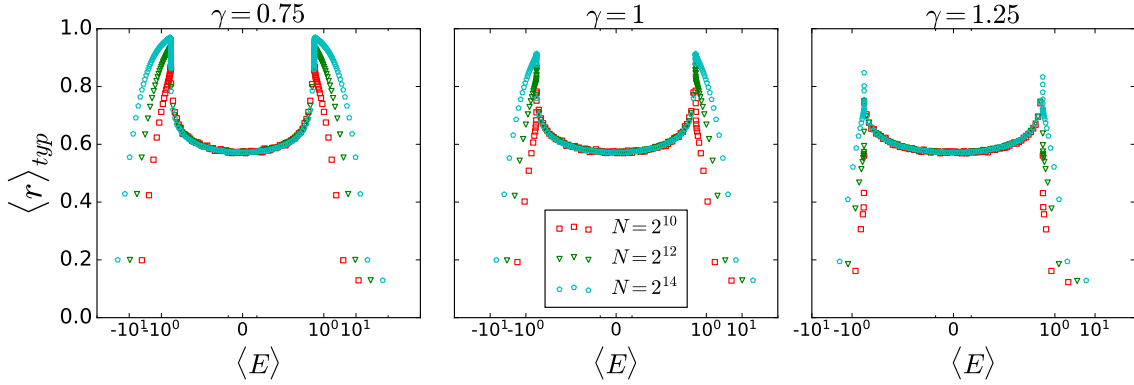


Figure 5: **The spectral ratio statistics $\langle r \rangle_{typ} = \exp \langle \ln r(E_n) \rangle$ versus energy $E_n$** in RDM model for $\gamma = 0.75$, 1, 1.25, $\theta = 0.25$, and $N = 2^{10}, 2^{12}, 2^{14}$. The data both for $r(E_n)$ and $E_n$ are averaged over 1000 realizations of disorder for each eigenvalue index separately.

delocalized phase, $\gamma < 2$, while non-ergodicity is visible only at higher order gap ratios (see, e.g., [29, 42, 43]) or other measures like spectral form factor, level compressibility [16] or power spectrum [44–46].

Figure 5 shows the conventional ratio statistics (47) across the spectrum in disordered RDM for $\gamma = 0.75$, 1, 1.25. One can see that, like in the Rosenzweig-Porter model, the ratio statistics in the bulk of the spectrum shows Wigner-Dyson unitary value $r_{GUE}$, while at the spectral edges the states correspond to the special $r$ values first going up to the equidistant spectrum $r = 1$ and then to the nearly degenerate values $r \simeq 0$.

The last measure of the wave-function spatial decay [12,27,29,47] uncovers the structure of the eigenstates followed from the effective Hamiltonian (34) and Eq. (35). In order to uncover the wave-function spatial decay we plot it versus the diagonal energy differences $|\varepsilon_m - \varepsilon_n|$, provided these energies are ordered $\varepsilon_n < \varepsilon_{n+1}$, see Fig. 6.

Indeed, according to (35), for the sites $n$, close in the diagonal energy $\varepsilon_n$ to the eigenvalue $E_m$, $|\varepsilon_n - E_m| \lesssim \Gamma$, the wave-function has a fractal structure $|\psi_{E_m}(n)|^2 \sim N^{-D}$ like in the Rosenzweig-Porter. This is confirmed by the Lorentzian form of the wave-function decay in Fig. 6, similar to the Rosenzweig-Porter results [47].
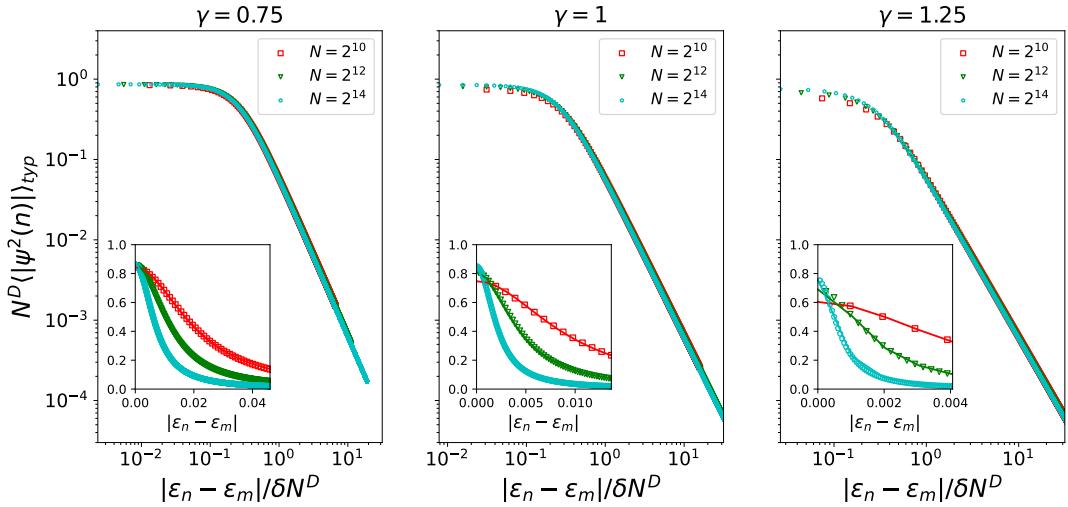
Figure 6: **The wave-function spatial decay** $N^D \left\langle |\psi_{E_m}(n)|^2 \right\rangle$ **versus the diagonal energy differences** $|\varepsilon_n - \varepsilon_m|$ in RDM model for $\gamma = 0.75$, 1, 1.25, $\theta = 0.25$, and $N = 2^{10}, 2^{12}, 2^{14}$. The data is averaged over 1000 realizations of disorder for each eigenvalue index separately. The main plots show the collapse of the curve with the rescaling $\delta \cdot N^D$ of the energy differences in the log-log scale. The insets show the linear scale without $x$-axis rescaling.

## 7 Conclusion and outlook

In this work we consider the localization and ergodicity-breaking properties of eigenstates in the disordered Russian Doll model, with the generalized amplitude of the coupling strength $\sim N^{-\gamma/2}$. We develop RG flow based on the renormalization of high-energy states in the momentum basis and provide the approximate solution for the effective Hamiltonian, valid for any number of the renormalized high-energy states within the considered parameter range.

In addition, we validate the above result and confirm the subleading character of the approximations by generalizing the matrix-inversion trick to the case of the spectrum of the off-diagonal hopping matrix, which is dense at all finite energies and divergent to both sides of the spectrum. This spectral structure corresponds to the phases of delocalized eigenstates that can be described by the above generalization of the matrix-inversion trick (cf. [14]).

Based on the effective Hamiltonian, we find the fractal dimension of the eigenstates in the spectral bulk and show that the non-ergodic phase of matter appears in the extended parameter range with respect to the Rosenzweig-Porter model and has different fractal dimension, $D = 1 - \gamma/2$.

Note that, as the fractal properties in RDM barely depend on the time-reversal symmetry breaking parameter $\theta \neq 0$, the Richardson model provides an example of an exceptional point, where the limiting behavior $\theta \to 0$ of the Russian Doll model does not correspond to the one of the Richardson model, $\theta = 0$. Unlike the case of the Burin-Maksimov model [12, 26, 27], where the symmetry-breaking parameter destroyed the BA integrability and, thus, the discontinuous character was expected, this work demonstrates that by breaking time-reversal symmetry, which keeps the model in the BA integrable class for any finite $N$ may lead to the same discontinuity. It would be also interesting to search for

the non-ergodicity in the ensemble of twisted XXX models with random inhomogeneities using the relation with the RDM model. Another interesting issue for further study concerns the derivation of the generalized RDM that is Richardson model with time-reversal symmetry breaking term and the generalized hopping term scaling, and the investigation of its fractal properties. It is an important direction of the research as already the generalized Richardson model describes the superconducting phase of the mixture of the Sachdev-Ye-Kitaev and the Fermi-Hubbard models [48].

Moreover, we show that the Russian Doll model provides an example of BA integrable model and delocalized non-ergodic eigenstates already in the single-particle sector. This consideration raises the question of the relation between BA integrability and the localization and opens a new avenue in this research direction.

## Acknowledgements

## A  Estimation of smallness of a parameter $S_{p,q}(2r)$ and $J_{p,q}(r) - \bar{J}_{p,q}(r)$

Within the condition (24), $r \ll r^{**} = N^{1-\gamma/3}$,

$$E_{p_r} \gg J_{p-q} \sim N^{-1/2} \tag{48}$$

and the sum $S_{p,q}(r)$, Eq. (23), is small compared to $J_{p-q}$

$$|S_{p,q}(2r)| \leq \left| \sum_{k=0}^{r} \frac{J_{p-p_k} J_{p_k-q}}{E_{p_k}} \right| \simeq \frac{1}{N^{1-\gamma/2}} \left| \frac{1}{N \cos\theta} + \frac{\pi}{2\sin\theta} \sum_{l=1}^{r} (2l-1) a_{p,q,l} \right| , \tag{49}$$

where $a_{p,q,l} = J_{p-2l+1} J_{2l-1-q} - J_{p+2l-1} J_{-2l+1-q}$ due to (9) has zero mean and the following variance

$$\langle a_{p,q,l} \rangle = 0 , \tag{50a}$$

$$\left\langle |a_{p,q,l}|^2 \right\rangle = \frac{2}{N^2} (1 + \delta_{p,q}) . \tag{50b}$$

Using this, the above sum of random variables can be approximated via its variance (as it have the zero mean)

$$\sum_{l=1}^{r} (2l-1)^2 \left\langle |a_{p,q,l}|^2 \right\rangle \simeq \frac{2r(4r^2-1)}{3N^2} (1 + \delta_{p,q}) . \tag{51}$$

Finally, this gives the following estimate for $S_{p,q}(2r)$ at $r \gg 1$

$$|S_{p,q}(2r)| \lesssim \frac{1}{N^{2-\gamma/2}} \left[ \frac{1}{\cos\theta} + \frac{r^{3/2}}{\sin\theta} \right] \ll J_{p-q} \simeq \frac{1}{N^{1/2}} , \tag{52}$$

due to $\gamma < 3$ and (24).

In the similar way one can estimate the difference

$$l_{p,q}(r) = J_{p,q}(r) - \bar{J}_{p,q}(r) , \quad l_{p,q}(1) = 0 . \tag{53}$$

Indeed, using Eqs. (19), (22), and (48) one immediately obtains

$$l_{p,q}(r+1) - l_{p,q}(r) \simeq \frac{1}{E_{p_r}} \left[ J_{p-p_k} \left( S_{p_k,q}(r) + l_{p_k,q}(r) \right) + J_{p_k-q} \left( S_{p,p_k}(r) + l_{p,p_k}(r) \right) \right] , \tag{54}$$

where we neglected the quadratic term $\left( S_{p,p_k}(r) + l_{p,p_k}(r) \right) \left( S_{p_k,q}(r) + l_{p_k,q}(r) \right)$ due to its smallness.

Further we estimate by the order of magnitude the parameter $l$ by rewriting the above equation for $l$ in the continuous form and neglecting the difference between variables with different indices

$$\frac{dl(r)}{dr} \simeq \frac{J}{E_{p_r}} \left( S(r) + l(r) \right) . \tag{55}$$

Solving this ordinary differential equation in the variable $x$

$$N^{-(3-\gamma)/2} \le x = \frac{Jr}{E_{p_r}} \sim \frac{r^2}{N^{(3-\gamma)/2}} \ll N^{(3-\gamma)/6} \tag{56}$$

one obtains

$$l(r) = -S(r) \frac{\int_0^x y^{3/4} e^y dy}{x^{3/4} e^x} . \tag{57}$$

For $x \ll 1$ one can immediately see that $|l(r)| \sim x S(r) \ll S(r)$.

In the opposite limit of $x \gtrsim 1$ one can only bound $|l(r)| \le S(r)$ using the condition for $y' = (x - y) \ge 0$ in the integrand

$$\left| \frac{l(r)}{S(r)} \right| = \int_0^x \left( 1 - \frac{y'}{x} \right)^{3/4} e^{-y'} dy' \le 1 . \tag{58}$$

In this case one cannot neglect $l(r)$ with respect to $S(r)$, but can absorb it to $S(r)$ if the numerical prefactors are not important. Thus, in the main text we consider both above cases of $x \ll 1$ and $x \gtrsim 1$.

# B  Derivation of the effective Hamiltonian (25) in the coordinate basis (27)

In Eq. (25) we separate our renormalized Hamiltonian in four terms

$$H_{p,q}^{(1)} = J_{p-q} , \quad H_{p,q}^{(2)} = \frac{J_p J_{-q}}{E_0} , \quad H_{p,q}^{(3)} = \sum_{l=1}^{r} \frac{a_{p,q,l}}{E_{2l-1}} , \quad H_{p,q}^{(4)} = E_q \delta_{p,q} , \tag{59}$$

where we introduce the notation $a_{p,q,l} = J_{p-2l+1} J_{2l-1-q} - J_{p+2l-1} J_{-2l+1-q}$ and $p, q \ne p_s$, with $0 \le s \le r$, and $p_s$ are from Eq. (21). The discrete Fourier transform of the above terms takes the form

$$H_{m,n}^{(k)} = \sum_{p,q \ne \{p_s\}} \frac{e^{\frac{2\pi i(pm-qn)}{N}}}{N} H_{p,q}^{(k)} = \left( \sum_{p,q} + \sum_{p,q=\{p_s\}} - \sum_{\substack{p, \\ q=\{p_s\}}} - \sum_{\substack{p=\{p_s\}, \\ q}} \right) \frac{e^{\frac{2\pi i(pm-qn)}{N}}}{N} H_{p,q}^{(k)} ,$$

$$\tag{60}$$

where we replaced the summation over $p, q \neq \{p_s\}$ by the complemented sums over the whole interval and over $p_s$ in either or both variables. The first summation is given just by the initial (not truncated) Fourier transform.

Here we will calculate all these terms one-by-one. The first term written in the above four sums takes the form

$$H_{m,n}^{(1)} = \sum_{p,q \neq \{p_s\}} \frac{e^{\frac{2\pi i(pm-qn)}{N}}}{N} J_{p-q} \equiv \varepsilon_m \delta_{mn} + i_{mn} - I_{mn} - K_{mn} \ , \tag{61}$$

where the first term corresponds to the diagonal disorder, the second one is given by

$$i_{mn} = \sum_{p,q=\{p_s\}} \frac{e^{\frac{2\pi i(pm-qn)}{N}}}{N} J_{p-q} \ , \tag{62}$$

while the last two terms are symmetric with respect to each other by the Hermitian conjugation

$$I_{mn} = \sum_{\substack{p, \\ q=\{p_s\}}} \frac{e^{\frac{2\pi i(pm-qn)}{N}}}{N} J_{p-q} = \sum_{\substack{p'=\{p_s\}, \\ q'}} \frac{e^{-\frac{2\pi i(p'n-q'm)}{N}}}{N} J_{q-p} = K_{nm}^* \tag{63}$$

with $p' = q$ and $q' = p$ and $J_{-p} = J_p^*$. Let's calculate, first, $I_{mn}$ by shifting the summation over $p$ to $k = p - q$

$$I_{mn} = \sum_{q=\{p_s\}} \frac{e^{\frac{2\pi iq(m-n)}{N}}}{N} \sum_k e^{\frac{2\pi ikm}{N}} J_k = \varepsilon_m \sum_{q=\{p_s\}} \frac{e^{\frac{2\pi iq(m-n)}{N}}}{N} = \varepsilon_m \left( \frac{1}{N} + \sum_{l=-r}^{r-1} \frac{e^{\frac{2\pi i(2l-1)(m-n)}{N}}}{N} \right) =$$

$$= \varepsilon_m \left( \frac{1}{N} + \frac{\sin\left(4\pi r(m-n)/N\right)}{N \sin\left(2\pi(m-n)/N\right)} \right) \ , \tag{64}$$

The second sum $i_{mn}$ in Eq. (61) can be found after the same shift

$$i_{mn} = \sum_{q=\{p_s\}} \frac{e^{\frac{2\pi iq(m-n)}{N}}}{N} \sum_{k+q=\{p_s\}} e^{\frac{2\pi ikm}{N}} J_k =$$

$$= \sum_{q=\{p_s\}} \frac{e^{\frac{2\pi iq(m-n)}{N}}}{N} g_{m,q} \sqrt{\frac{r}{N}} \lesssim \left( \frac{1}{N} + \frac{\sin\left(4\pi r(m-n)/N\right)}{N \sin\left(2\pi(m-n)/N\right)} \right) g_{m,q} \sqrt{\frac{r}{N}} \ll I_{mn} \tag{65}$$

and estimating the following sum with the random phase approximation

$$\sum_{k=\{p_s-q\}} e^{\frac{2\pi ikm}{N}} J_k \simeq g_{m,q} \sqrt{\frac{r}{N}} \tag{66}$$

and the central limit theorem for $r \gg 1$ leading to random variable $g_m$ of the order of one.

After neglecting of the small terms $g_m \sqrt{r/N}$ with respect to $\varepsilon_m$ we obtain for the first term

$$H_{m,n}^{(1)}(2r) \simeq \varepsilon_m \delta_{mn} - (\varepsilon_m + \varepsilon_n) \frac{\sin\left(4\pi r(m-n)/N\right)}{N \sin\left(2\pi(m-n)/N\right)} \sim$$

$$\sim \varepsilon_m \delta_{mn} - (\varepsilon_m + \varepsilon_n) \begin{cases} \frac{r}{N}, & |m-n| \leq \frac{N}{r} \\ \frac{\sin(4\pi r(m-n)/N)}{2\pi|m-n|}, & |m-n| \geq \frac{N}{r} \end{cases} \ . \tag{67}$$

In the last equality we approximate the sine factors of the last term by linear functions when their arguments are small compared to one.

The second term $H_{m,n}^{(2)}$ splits in the product of two equivalent sums, giving in the same approximation as for $i_{mn}$

$$
\left(N^{2-\gamma/2}\cos\theta\right)H_{m,n}^{(2)} = \sum_{p,q\neq\{p_s\}} e^{\frac{2\pi i(pm-qn)}{N}} J_p J_{-q} = \sum_{p\neq\{p_s\}} e^{\frac{2\pi ipm}{N}} J_p \sum_{q\neq\{p_s\}} e^{\frac{2\pi iqn}{N}} J_{-q} \simeq
$$

$$
\simeq \left(\varepsilon_m - g_{m,0}\sqrt{\frac{r}{N}}\right)\left(\varepsilon_n - g_{n,0}\sqrt{\frac{r}{N}}\right) \sim \varepsilon_m \varepsilon_n . \quad (68)
$$

The third term $H_{m,n}^{(3)}$ within the same approximation reads as

$$
\left(\frac{2}{\pi}N^{2-\gamma/2}\sin\theta\right)H_{m,n}^{(3)} = \sum_{p,q\neq\{p_s\}} e^{\frac{2\pi i(pm-qn)}{N}} \sum_{l=1}^{r}(2l-1)\left(J_{p-2l+1}J_{2l-1-q} - J_{p+2l-1}J_{-2l+1-q}\right) =
$$

$$
= \sum_{l=1}^{r}(2l-1)\left[e^{\frac{2\pi i(2l-1)(m-n)}{N}}\left(\varepsilon_m - g_{m,2l-1}\sqrt{\frac{r}{N}}\right)\left(\varepsilon_n - g_{n,2l-1}^*\sqrt{\frac{r}{N}}\right) - \right.
$$

$$
\left. - e^{-\frac{2\pi i(2l-1)(m-n)}{N}}\left(\varepsilon_m - g_{m,2l-1}^*\sqrt{\frac{r}{N}}\right)\left(\varepsilon_n - g_{n,2l-1}\sqrt{\frac{r}{N}}\right)\right] \simeq
$$

$$
\simeq 2i\varepsilon_m\varepsilon_n\sum_{l=1}^{r}(2l-1)\sin\left[\frac{2\pi}{N}(2l-1)(m-n)\right] \sim
$$

$$
\sim 2i\varepsilon_m\varepsilon_n \begin{cases} \frac{r(4r^2-1)}{3}\frac{2\pi(m-n)}{N}, & |m-n| \ll \frac{N}{r} \\ c\frac{N^2\mathrm{sign}(m-n)}{(m-n)^2} + 2r - \frac{N}{\pi(m-n)}, & |m-n| \gg \frac{N}{r} \end{cases} \quad (69)
$$

In the last case we assumed that sine of the large argument is more or less equivalent to $(-1)^l$. In both latter derived equations we again used (66) and neglected these terms with respect to $\varepsilon_m$.

The last term is given by the truncated initial hopping term which we do not split into the above four sums (60):

$$
H_{m,n}^{(4)} = \sum_{p\neq\{p_s\}} \frac{e^{\frac{2\pi ip(m-n)}{N}}}{N} E_p = \frac{2}{\pi}N^{-\gamma/2}\sin\theta\sum_{k=r}^{N/2}\frac{\sin\left[\frac{2\pi}{N}(2k-1)(m-n)\right]}{2k-1} . \quad (70)
$$

Again using the same approximation for sine of the large argument as $(-1)^k$ we will obtain

$$
H_{m,n}^{(4)} \sim \frac{2}{\pi}N^{-\gamma/2}\sin\theta \begin{cases} \left(1 - r\frac{m-n}{N}\right) + c\frac{m-n}{N}, & |m-n| \ll \frac{N}{r} \\ \frac{c}{r} - \frac{2c}{N}, & |m-n| \gg \frac{N}{r} \end{cases} \quad (71)
$$

The first bracket in the first case corresponds to the small argument of the sine, $k \leq N/[4\pi(m-n)]$, while the rest terms correspond to the large sine argument.

To sum up, in the coordinate basis at $2r$th step we have the following estimate for the renormalized Hamiltonian given in Eq. (27)

$$
H_{m,n}(2r) \sim \varepsilon_m\delta_{mn} + \frac{\varepsilon_m\varepsilon_n}{N^{2-\gamma/2}\cos\theta} +
$$

$$
+ \begin{cases} \frac{2}{\pi}N^{-\gamma/2}\sin\theta\left(1 - r\frac{m-n}{N}\right) + \frac{i8\pi^2\varepsilon_m\varepsilon_n(m-n)r^3}{3N^{3-\gamma/2}\sin\theta} - (\varepsilon_m + \varepsilon_n)\frac{r}{N}, & |m-n| \ll \frac{N}{r} \\ \frac{2}{\pi}N^{-\gamma/2}\sin\theta\frac{c}{r} + \frac{i2\pi\varepsilon_m\varepsilon_n}{N^{2-\gamma/2}\sin\theta}\left(c\frac{N^2\mathrm{sign}(m-n)}{(m-n)^2} + r\right) - \frac{\varepsilon_m+\varepsilon_n}{2\pi|m-n|}, & |m-n| \gg \frac{N}{r} \end{cases} , \quad (72)
$$

with $1 \leq r \leq N/4$ and a certain unimportant constant $c$.

## C   Extrapolation of the multifractality measures to the thermodynamic limit $N \to \infty$

Here we remind the standard extrapolation procedure for the spectrum of fractal dimensions (see, e.g., [12, 13, 16, 27, 38]) and for the fractal dimensions $D_q$ [37].

For the first one we express the multifractal spectrum $f(\alpha, N)$ at finite system size $N$

$$f(\alpha, N) = f(\alpha) + \frac{A_\alpha^{(1)}}{\ln N} + \frac{A_\alpha^{(2)}}{(\ln N)^2} + \dots \, , \tag{73}$$

with certain constants $A_\alpha^{(k)}$ depending on $\alpha$. The latter expression can be derived using the definition Eq. (38) and extracted directly from the histogram over $\alpha$ [12, 16, 38, 39]. Here and further we stick to the simplest linear in $1/\ln N$ behavior, which is typical for the models with fractal eigenstates [12, 14, 16].
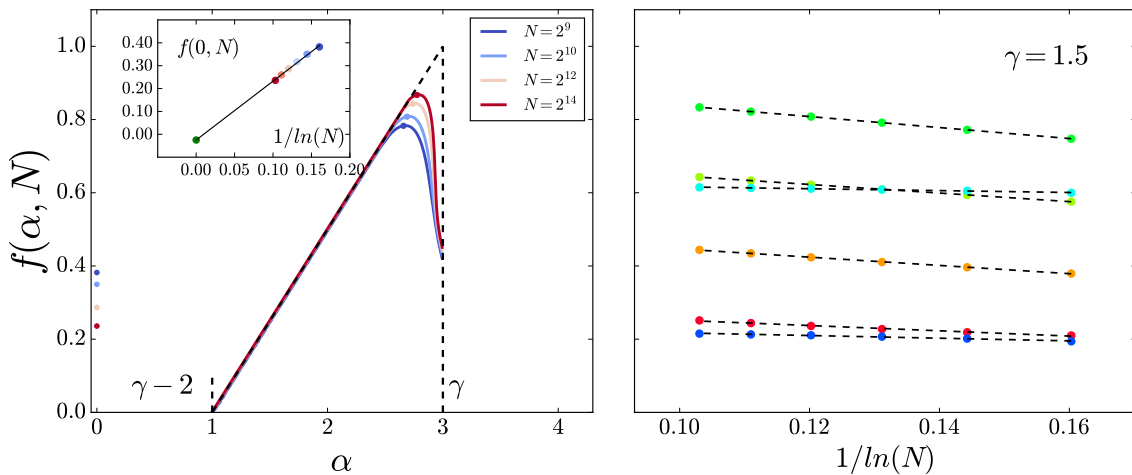


Figure 7: **Finite-size extrapolation of the multifractal spectrum** $f(\alpha)$ for 50 % mid-spectrum eigenstates and $\theta = 0.25$. (left) $f(\alpha, N)$ and its extrapolation for $\gamma = 3$, the inset shows the extrapolation of $f(0, N)$ vs $1/\ln N$, (right) extrapolation of $f(\alpha, N)$ vs $1/\ln N$ at $\gamma = 1.5$ for several values of $\alpha$. $f(\alpha)$ is extrapolated from $N = 2^9 - 2^{14}$ with 1000 disorder realizations for each $\gamma$ value.

The corresponding finite-size $f(\alpha, N)$ and extrapolated $f(\alpha)$ curves are given in Fig. 7 for 50 % of mid-spectrum states. As an additional marker of the extrapolation quality we check that the normalization condition, $\max_\alpha f(\alpha) = f(\alpha_0) = 1$, of the probability distribution $\mathcal{P}(\alpha)$ is satisfied.

The finite-size fractal dimension is defined by the formula (42) $D_q(N) = \ln I_q / (1 - q) \ln N$, with the generalized inverse participation ratio (IPR),

$$I_q = \sum_i |\psi_n(i)|^{2q} = c_q N^{(1-q)D_q} \, . \tag{74}$$

In order to avoid the parasitic contributions from measure zero of special eigenstates we focus on the typical averaging of the IPR both over the disorder and the eigenstates

$$I_{q,typ} = e^{\langle \ln I_q \rangle} \sim N^{-(q-1)D_{q,typ}} \tag{75}$$

and omit the subscript "typ" for brevity.
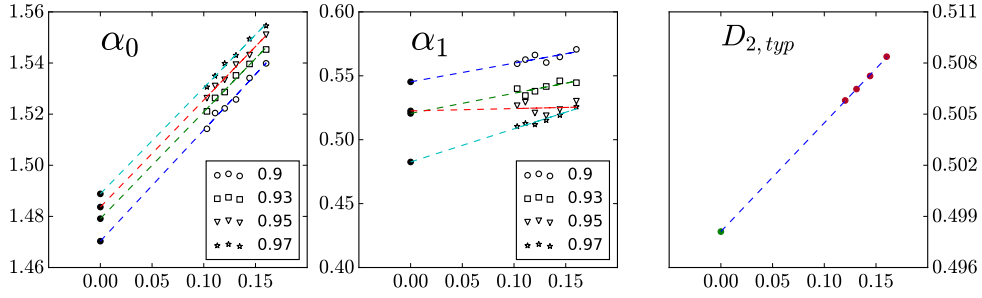
Figure 8: **Finite-size extrapolation of the fractal dimension** $\alpha_0$, $\alpha_1$ and $D_2$ for $\gamma = 1$, $\theta = 0.25$. $D_2$ is extrapolated from the same system sizes as $f(\alpha)$ in Fig. 7. Different symbols in the extrapolation of $\alpha_q$ correspond to different percentage $P$ of the deviation from the maximum of the function $f(\alpha_q) - q\alpha_q$ used for the extrapolation.

As the main contribution to IPR is given by the scaling exponent $D_q$ and the prefactor $c_q$ similarly to (73) one obtains

$$D_q(N) = D_q + \frac{(1-q)^{-1}\ln c_q}{\ln N} \ . \tag{76}$$

The extrapolation of $D_q(N)$ vs $1/\ln N$ extracted from $I_2$ and from $\alpha_0$ and $\alpha_1$ is shown in Fig. 8. Here in order to diminish finite $\alpha$-bin size for extracting $\alpha_q$ we fit $f(\alpha) - q\alpha$ close to its maximum with a parabolic fit and associate $\alpha_q$ with the maximal position of this fit. The fitting interval, $\alpha_- \leq \alpha \leq \alpha_+$, is determined by the deviation from the maximal value $f(\alpha_q) - q\alpha_q$ to

$$f(\alpha_\pm) - q\alpha_\pm = (f(\alpha_q) - q\alpha_q) P \ , \tag{77}$$

with the percentage $P = 0.9, 0.93, 0.95, 0.97$ shown in the legends of Fig. 8. One can straightforwardly see that 7 % change in $P$ affects the extrapolation by at most the same amount. The same procedure is done for $\alpha_0(N)$ and $\alpha_1(N)$ mentioned in Eqs. (39) and (44).

# References

[1] R. Richardson, *A restricted class of exact eigenstates of the pairing-force Hamiltonian*, Phys. Lett. **3**(6), 277 (1963), doi:10.1016/0031-9163(63)90259-2.

[2] R. Richardson and N. Sherman, *Exact eigenstates of the pairing-force Hamiltonian*, Nuclear Physics **52**, 221 (1964), doi:10.1016/0029-5582(64)90687-X.

[3] M. C. Cambiaggio, A. M. F. Rivas and M. Saraceno, *Integrability of the pairing hamiltonian*, Nuclear Physics A **624**(2), 157 (1997), doi:10.1016/S0375-9474(97)00418-1.

[4] A. Ossipov, *Anderson localization on a simplex*, J. Phys. A **46**, 105001 (2013), doi:10.1088/1751-8113/46/10/105001.

[5] R. Modak, S. Mukerjee, E. A. Yuzbashyan and B. S. Shastry, *Integrals of motion for one-dimensional Anderson localized systems*, New J. Phys. **18**, 033010 (2016), doi:10.1088/1367-2630/18/3/033010.

[6] M. L. Mehta, *Random matrices*, Elsevier, doi:10.1016/C2009-0-22297-5 (2004).

[7] A. LeClair, J. María Román and G. Sierra, *Russian doll renormalization group and superconductivity*, Phys. Rev. B **69**, 020505 (2002), doi:10.1103/PhysRevB.69.020505.

[8] A. LeClair, J. M. Román and G. Sierra, *Russian doll renormalization group and Kosterlitz-Thouless flows*, Nucl. Phys. B **675**(3), 584 (2003), doi:10.1016/j.nuclphysb.2003.09.032.

[9] C. Dunning and J. Links, *Integrability of the Russian doll BCS model*, Nucl. Phys. B **702**(3), 481 (2004), doi:10.1016/j.nuclphysb.2004.09.021.

[10] M. Asorey, F. Falceto and G. Sierra, *Chern-Simons theory and BCS superconductivity*, Nucl. Phys. B **622**(3), 593 (2002), doi:10.1016/S0550-3213(01)00614-9.

[11] K. M. Bulycheva and A. S. Gorskii, *Limit cycles in renormalization group dynamics*, Phys. Usp. **57**(2), 171 (2014), doi:10.3367/UFNe.0184.201402g.0182.

[12] P. A. Nosov, I. M. Khaymovich and V. E. Kravtsov, *Correlation-induced localization*, Phys. Rev. B **99**(10), 104203 (2019), doi:10.1103/PhysRevB.99.104203.

[13] P. A. Nosov and I. M. Khaymovich, *Robustness of delocalization to the inclusion of soft constraints in long-range random models*, Phys. Rev. B **99**, 224208 (2019), doi:10.1103/PhysRevB.99.224208.

[14] A. G. Kutlin and I. M. Khaymovich, *Emergent fractal phase in energy stratified random models*, SciPost Phys. **11**, 101 (2021), doi:10.21468/SciPostPhys.11.6.101.

[15] N. Rosenzweig and C. E. Porter, *Repulsion of energy levels" in complex atomic spectra*, Phys. Rev. B **120**, 1698 (1960), doi:10.1103/PhysRev.120.1698.

[16] V. E. Kravtsov, I. M. Khaymovich, E. Cuevas and M. Amini, *A random matrix model with localization and ergodic transitions*, New J. Phys. **17**, 122002 (2015), doi:10.1088/1367-2630/17/12/122002.

[17] S. Roy, I. M. Khaymovich, A. Das and R. Moessner, *Multifractality without fine-tuning in a Floquet quasiperiodic chain*, SciPost Phys. **4**, 25 (2018), doi:10.21468/SciPostPhys.4.5.025.

[18] W. Tang and I. M. Khaymovich, *Non-ergodic delocalized phase with poisson level statistics*, doi:10.48550/ARXIV.2112.09700 (2021).

[19] C. Monthus, *Multifractality of eigenstates in the delocalized non-ergodic phase of some random matrix models: Wigner-Weisskopf approach*, J. Phys. A: Math. Theor. **50**, 295101 (2017), doi:10.1088/1751-8121/aa5ad2.

[20] V. E. Kravtsov, I. M. Khaymovich, B. L. Altshuler and L. B. Ioffe, *Localization transition on the random regular graph as an unstable tricritical point in a log-normal rosenzweig-porter random matrix ensemble*, doi:10.48550/ARXIV.2002.02979 (2020).

[21] I. M. Khaymovich, V. E. Kravtsov, B. L. Altshuler and L. B. Ioffe, *Fragile extended phases in the log-normal Rosenzweig-Porter model*, Phys. Rev. Research **2**, 043346 (2020), doi:10.1103/PhysRevResearch.2.043346.

[22] I. M. Khaymovich and V. E. Kravtsov, *Dynamical phases in a "multifractal" Rosenzweig-Porter model*, SciPost Phys. **11**, 45 (2021), doi:10.21468/SciPostPhys.11.2.045.

[23] G. Biroli and M. Tarzia, *Lévy-Rosenzweig-Porter random matrix ensemble*, Phys. Rev. B **103**, 104205 (2021), doi:10.1103/PhysRevB.103.104205.

[24] A. G. Kutlin and I. M. Khaymovich, *Multifractal phase in real and energy spaces*, in preparation (2022).

[25] G. De Tomasi and I. M. Khaymovich, *Non-Hermitian Rosenzweig-Porter random-matrix ensemble: Obstruction to the fractal phase*, doi:10.48550/ARXIV.2204.00669 (2022).

[26] A. L. Burin and L. A. Maksimov, *Localization and delocalization of particles in disordered lattice with tunneling amplitude with $r^{-3}$ decay*, JETP Lett. **50**, 338 (1989).

[27] X. Deng, V. E. Kravtsov, G. V. Shlyapnikov and L. Santos, *Duality in power-law localization in disordered one-dimensional systems*, Phys. Rev. Lett. **120**(11), 110602 (2018), doi:10.1103/PhysRevLett.120.110602.

[28] A. G. Kutlin and I. M. Khaymovich, *Renormalization to localization without a small parameter*, SciPost Phys. **8**, 49 (2020), doi:10.21468/SciPostPhys.8.4.049.

[29] X. Deng, A. L. Burin and I. M. Khaymovich, *Anisotropy-mediated reentrant localization*, doi:10.48550/ARXIV.2002.00013 (2020).

[30] L. S. Levitov, *Absence of localization of vibrational modes due to dipole-dipole interaction*, Europhys. Lett. **9**, 83 (1989), doi:10.1209/0295-5075/9/1/015.

[31] L. S. Levitov, *Delocalization of vibrational modes caused by electric dipole interaction*, Phys. Rev. Lett. **64**, 547 (1990), doi:10.1103/PhysRevLett.64.547.

[32] E. Bogomolny and M. Sieber, *Eigenfunction distribution for the Rosenzweig-Porter model*, Phys. Rev. E **98**, 032139 (2018), doi:10.1103/PhysRevE.98.032139.

[33] G. D. Tomasi, M. Amini, S. Bera, I. M. Khaymovich and V. E. Kravtsov, *Survival probability in generalized Rosenzweig-Porter random matrix ensemble*, SciPost Phys. **6**, 14 (2019), doi:10.21468/SciPostPhys.6.1.014.

[34] V. Motamarri, A. S. Gorsky and I. M. Khaymovich, *Breaking of a periodic renormalization group in russian doll model by disorder*, in preparation (2022).

[35] A. D. Mirlin, Y. V. Fyodorov, F.-M. Dittes, J. Quezada and T. H. Seligman, *Transition from localized to extended eigenstates in the ensemble of power-law random banded matrices*, Phys. Rev. E **54**, 3221 (1996), doi:10.1103/PhysRevE.54.3221.

[36] E. Bogomolny and O. Giraud, *Perturbation approach to multifractal dimensions for certain critical random-matrix ensembles*, Phys. Rev. E **84**, 036212 (2011), doi:10.1103/PhysRevE.84.036212.

[37] F. Evers and A. D. Mirlin, *Anderson transitions*, Rev. Mod. Phys **80**, 1355 (2008), doi:10.1103/RevModPhys.80.1355.

[38] A. De Luca, B. L. Altshuler, V. E. Kravtsov and A. Scardicchio, *Anderson localization on the Bethe lattice: Nonergodicity of extended states*, Phys. Rev. Lett. **113**(4), 046806 (2014), doi:10.1103/PhysRevLett.113.046806.

[39] D. J. Luitz, I. M. Khaymovich and Y. Bar Lev, *Multifractality and its role in anomalous transport in the disordered XXZ spin-chain*, SciPost Phys. Core **2**, 6 (2020), doi:10.21468/SciPostPhysCore.2.2.006.

[40] V. Oganesyan and D. A. Huse, *Localization of interacting fermions at high temperature*, Phys. Rev. B **75**, 155111 (2007), doi:10.1103/PhysRevB.75.155111.

[41] Y. Y. Atas, E. Bogomolny, O. Giraud and G. Roux, *Distribution of the ratio of consecutive level spacings in random matrix ensembles*, Phys. Rev. Lett. **110**, 084101 (2013), doi:10.1103/PhysRevLett.110.084101.

[42] Y. Y. Atas, E. Bogomolny, O. Giraud, P. Vivo and E. Vivo, *Joint probability densities of level spacing ratios in random matrices*, Journal of Physics A: Mathematical and Theoretical **46**(35), 355204 (2013), doi:10.1088/1751-8113/46/35/355204.

[43] S. H. Tekur, U. T. Bhosale and M. S. Santhanam, *Higher-order spacing ratios in random matrix theory and complex quantum systems*, Phys. Rev. B **98**, 104305 (2018), doi:10.1103/PhysRevB.98.104305.

[44] R. Berkovits, *Super-Poissonian behavior of the Rosenzweig-Porter model in the nonergodic extended regime*, Phys. Rev. B **102**, 165140 (2020), doi:10.1103/PhysRevB.102.165140.

[45] R. Berkovits, *Probing the metallic energy spectrum beyond the thouless energy scale using singular value decomposition*, Phys. Rev. B **104**, 054207 (2021), doi:10.1103/PhysRevB.104.054207.

[46] L. Colmenarez, D. J. Luitz, I. M. Khaymovich and G. De Tomasi, *Subdiffusive thouless time scaling in the anderson model on random regular graphs*, Phys. Rev. B **105**, 174207 (2022), doi:10.1103/PhysRevB.105.174207.

[47] W. Buijsman and Y. B. Lev, *Circular Rosenzweig-Porter random matrix ensemble*, SciPost Phys. **12**, 82 (2022), doi:10.21468/SciPostPhys.12.3.082.

[48] H. Wang, A. L. Chudnovskiy, A. Gorsky and A. Kamenev, *Sachdev-ye-kitaev superconductivity: Quantum kuramoto and generalized richardson models*, Physical Review Research **2**(3) (2020), doi:10.1103/physrevresearch.2.033025.